Mobile Broadband Radio Communications: Physical Aspects

José Fernandes

Resumo — **Este artigo aborda os aspectos da modelação do canal de propagação na banda das ondas milimétricas e seu impacto no desempenho de transmissão do sistema de comunicação rádio móvel de banda larga que pretende estender aos utilizadores móveis os serviços previstos para a Rede Digital com Integração de Serviços de Banda Larga. Conclui-se que com um esforço de equalização moderado é possível atingir algumas dezenas, ou até centenas de Mbit/s por portadora, desde que se escolha uma configuração de antenas adequada ao cenário onde se pretende instalar o sistema.**

Abstract — **This paper deals with the propagation channel modeling aspects in the millimeter-wave band and its impact on the transmission performance of a mobile broadband radio communication system that intends to extend to the mobile users the range of services envisioned for the B-ISDN. It concludes that with a low equalization effort is possible to achieve some tens or even hundreds of Mbit/s per carrier provided an adequate antenna configuration for the environment is chosen.**

I. INTRODUCTION

The Alexander Bell experiments dictate the beginning of the telecommunications industry and open the way for a new era in the human history. Those experiments drove the progressive development of technologies that will culminate with the global inter-connection of the information networks. The technology has progressing from switching circuits to the packet switching, from copper wires to the optical fibers, satellites and mobile communications. The telecommunications became the most important global stimulus for the economy growth.

The mobile communications constitute, at the same time, a tool and a weapon. As a tool, it enables the construction of a global and ubiquitous communication infra-structure; as a weapon, they are the competitiveness key for those who trade in the world-wide market. They are already considered as a business of the century and the number of users has been increasing dramatically. The Personal communications has the potential to reach a penetration of 80% while telephones connected to the fixed network are not expected to reach more than 50% of the population.

The advanced technological developments has permitted the continuous terminal miniaturization and increasing the functionality's, such as, terminals with touchscreen facilities, PCMCIA cards inside the terminals, multifunction terminals which acts as a normal phone and enables to send and receive e-mail messages, faxes, access to the Internet and also the normal functions of an organizer.

The actual systems have several limitations that will be overcome in future. One is the low data rate transmission capacity, 9.6 kbit/s for GSM (Global System for Mobile communications). The UMTS (Universal Mobile Telecommunications System) offers a data rate up to 2 Mbit/s and it will be available in the next decade. On the other hand, the increasing data rate requirements to support wide band services, makes the 2 Mbit/s supported by UMTS insufficient.

The baseline work towards a mobile broadband system (MBS) was carried out under RACE (Research and development in Advanced Communications technologies in Europe) program within R2067 MBS project [1]. This project starts in 1992, had a duration of four years and it has concentrated on market aspects, services and applications, technological and systems aspects. It also developed the necessary components and built a demonstrator which has proved that is possible to transmit image through a mobile radio link at 16 Mbit/s. The MBS concept is basically to extend the wide-band services available in the fixed network to the mobile users. This implies to establish a system configuration able to support a variety of equipment, services and applications that need high data transmission rates at fair costs. In this context it is possible the full integration with the B-ISDN (Broadband Integrated Services Digital Network).

The MBS does not pretend to become a cellular system to cover wide areas, neither to replace UMTS. The first application scenarios envisaged for the MBS are the zones with high traffic density where the user requires data rates higher than 2 Mbit/s. This type of system is well suited for private communication networks (PCN), especially for professional applications. The interconnection of several PCNs, in a city or industrial area, will constitute the first public MBS. Its extension along the main streets, will make the MBS as a general use system in urban and industrial centers [1].

In this context, the European Commission is now partially funding, under the ACTS (Advanced Communications Technologies and Services) program, the SAMBA project (System for Advanced Mobile Broadband Applications) which intends to continue the

promotion of the MBS concept and the development of the mobile broadband cellular systems. The SAMBA project focus mainly on the development and implementation of a demonstrator with more functionality's. Two simultaneous ATM (Asynchronous Transfer Mode) bi-directional links with a user bit rate of 34 Mbit/s will be implemented using the 40 GHz band including the handover functionality taking into account the radio and network aspects.

There are significant activities world-wide concerning the mobile broadband communications, namely in Europe, Australia, Canada and Japan, but most of them aim the wireless local area networks (WLAN) with bit rates up to 155 Mbit/s, for indoor environments[2]-[5].

The standardization bodies, namely the ATM Forum and ETSI (European Telecommunications Standards Institute), are also paying attention to this fact and already set up working groups to achieve consensus in this field. The first one is particularly involved with mobility management and medium access techniques. The activities on identification of the WLAN requirements have already started.

No matter what standard that will be approved for the mobile broadband communications and wireless access, the transmission medium will be the free space using the frequency band more convenient among the available spectrum. As the wide-band services require large band width, the only possibility is to use the millimeter-wave (mmw) band due to the congestion of the lower bands. In this context, the 62-63 GHz and 65-66 GHz as well as the 39.5-40.5 GHz and 42.5-43.5 GHz bands were provisionally allocated.

The propagation mechanisms of the electromagnetic waves are complex making the propagation channel not easy to characterize. The primary requisite to maintain a reliable link is to guarantee a certain power level within the coverage area. On the other hand, the movement of the terminals along the streets and inside buildings, etc., makes the channel time variant and dispersive due to the received replicas of the transmitted signal, causing inter-symbol interference (ISI) degrading the transmission quality. The channel characterization is therefore of high importance to allow an adequate choice of the modulation and coding schemes and signal processing techniques to mitigate the signal distortions introduced by the transmission channel.

II. MMW CHANNEL MODELING

The possibility of using the mmw band as a transmission medium for mobile broadband communications has been emphasized recently. Despite the efforts that have been done[6]-[14], a precise characterization of the propagation channel using this frequency band is still not available. In order to attain insight into the characteristics of mmw channels, extensive measurement campaigns are necessary. As this is a very time consuming and expensive task, it is realistically impossible to make measurements with all kinds of antennas within all kinds of scenarios. On the other hand, a computer program, able to simulate the multipath propagation phenomena, can be used to estimate the impulse response of the propagation channel in a given scenario, provided that it had been extensively validated with measurements and proved to be reliable [6].

Ray-tracing tools have proved to be very suitable for radio channel modeling[15]. Such a tool can be very helpful in studying the impact of the transceiver antennas and respective configuration (radiation pattern, polarization, location of the base station, etc.) in the channel impulse response. This can help the implementation and designing system engineers with a better knowledge concerning the propagation channel when making their decisions and optimizing their solutions.

The propagation channel is the part of the system seen between the transmitter and receiving antenna. The effect of the channel can be compared to a linear filter that causes distortion on the transmitted signal and can be described in the time or frequency domain. The time domain description is more informative, once it gives the amplitude and the excess time delay information of the multipath components which are generally complex and time variant due to the movements in the propagation scenario. The received signal is therefore the sum of all contributing multipath components which enables to describe the channel as a two port filter with random and time variant characteristics. Thus, the channel impulse response can be described by the theory of the linear time variant channels [16].

Considering a deterministic time variant channel, with a complex envelop response of the equivalent filter $h(t,\tau)$, where τ and t are the delay and time variables respectively, the complex envelop $w(t)$ at the output of the filter is related with the complex envelop signal at the input by:

$$w(t) = \int_{-\infty}^{+\infty} z(t-\tau)h(t,\tau)d\tau \qquad (1)$$

Physically, $h(t,\tau)$ can be seen as the channel response in time t to a pulse delayed by τ seconds. Each pulse can be seen as a result of the scattering of the transmitted signal in an obstacle, producing amplitude fluctuation $h(t,\tau)d\tau$ with a delay difference of $d\tau$. Writing (1) in the discrete form, results the eq. (2) [17]:

$$w(t) = \Delta\tau \sum_{n=0}^{N} z(t-n\Delta\tau)h(t,n\Delta\tau) \qquad (2)$$

and is represented in Fig. 1 as a tapped-delay-line, which is similar to a FIR (Finite Impulse Response) filter.

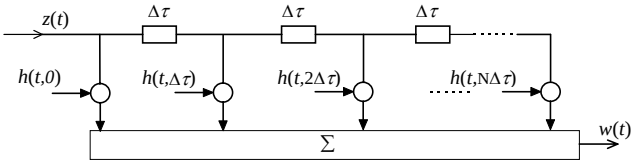

Fig. 1 Impulse response of time variant multipath channel represented as a tapped-delay-line

In practice the fading statistics of a mobile radio channel can be characterized as stationary in small time intervals or small areas. However the channel is not strictly stationary, but Wide-Sense Stationary (WSS) or weakly stationary. One important property of this type of channels is that the auto-correlation function is invariant to a time translation, i.e., the fading statistics do not change significantly in a time interval ξ.

A propagation environment with several obstacles, originates different replicas of the transmitted signal with excess time delay and Doppler shifts. The individual contributions are not correlated if they produce different Doppler shifts or if they have a different path lengths, leading to the definition of the Uncorrelated Scattering (US) channel. Combining both properties, results a class of Wide-Sense Stationary Uncorrelated Scattering (WSSUS) channels. This is the simpler class of time variant channels and fortunately the mobile radio channels belong to this category.

The WSSUS channels can be represented by a group of a non scintillate scatters, each one identifying a path, distinguished in time by its path length and in Doppler shift domain by its arriving angle to the receiver. The delay-Doppler power spectral density, $P_S(\tau,\nu)$, for this type of channels can be identified as a bidimensional scattering function. The power spectral density, $P_h(\xi;\tau)$, can be obtained by summing up all components of the Doppler shift and can be related with $h(t,\tau)$ trough the following equation[17]:

$$P_h(\xi;\tau) = E\left[h(t,\tau)h^*(t+\xi,\tau)\right] \qquad (3)$$

In mobile radio channels, the $E[|h(t,\tau)|^2]$ can be obtained through the measurement of $h(t,\tau)$ along a short path or small area. The graphic representation of the echoes power as a function of the excess time delay is named power delay profile (PDP) and represents the amplitude of the different multipath components seen by the receiver antenna. Usually the origin is set equal to zero ($\tau = 0$) at the arriving time of the first echo (shortest path). When the observation time interval tends to zero, $\xi = 0$, i.e., the channel is invariant in a short time, then $P_h(\xi;\tau) = P_h(\tau)$. Three relevant statistical parameters for the system design are the average mean delay ($\bar{\tau}$), the rms delay spread (DS) and the delay window (DW). The $\bar{\tau}$ is the first and the DS is the second central moment of the $P_h(\tau)$, respectively defined by [17]:

$$\bar{\tau} = \frac{\int_0^\infty \tau P_h(\tau)d\tau}{\int_0^\infty P_h(\tau)d\tau} \qquad (4)$$

$$DS = \sqrt{\frac{\int_0^\infty \left(\tau-\bar{\tau}\right)^2 P_h(\tau)d\tau}{\int_0^\infty P_h(\tau)d\tau}} \qquad (5)$$

The mean delay is related with the phase error while the DS gives an indication of the potential ISI which limits the carrier bit rate. The DW (at x%) is defined as the length of the middle portion of the PDP containing a certain percentage of the total energy of the PDP, and is given by

$$DW = \tau_2 - \tau_1 \qquad (6)$$

where τ_1 and τ_2 are defined as:

$$\int_{\tau_1}^{\tau_2} P_h(\tau)d\tau = x\int_{\tau_0}^{\tau_3} P_h(\tau)d\tau = xP_{tot} \qquad (7)$$

and τ_0 and τ_3 are, respectively, the instant where $P_h(\tau)$ exceeds a certain threshold (defined by the noise and interference level) and when it goes below that threshold.

Another parameter, not less important, is the attenuation introduced by the channel, and is defined by the received to the transmitted power ratio, that we call normalized received power (NRP)

$$PRN = \frac{P_r}{P_t} = \frac{\int_0^\infty P_h(\tau)d\tau}{\int_0^\infty |u(\tau)|^2 d\tau} \qquad (8)$$

with $u(\tau)$ being the transmitted pulse.

The mobile radio channel is wide sense stationary in a short time interval or small area, but for larger distances, it is time variant due to the scenario and mobile terminal movements which requires a non-stationary characterization. However, it is possible to use successively small scale statistics to characterize the channel in wide areas. This can be done through the calculation of the small scale statistical parameters (e.g., $\bar{\tau}$ and DS) to obtain the distribution of those parameters in the area of interest. Although this method permits to obtain useful parameters for system design, they represent only static measurements of the channel. A more powerful and more useful characterization is to model physically the channel, thus enabling to simulate the global system performance based on a realistic description of the propagation channel[6]-[10].

As in indoor environments the mobile terminals are stationary or slow moving during the communication, the Doppler effect can be neglected, and the most adequate function to characterize the radio channel is $h(t,\tau)$, with its discrete version given by [20]:

$$h(t,\tau) = \sum_{n=0}^{N} \alpha_n(t)\delta\left[\tau - \tau_n(t)\right]e^{j\varphi_n(t)} \qquad (9)$$

with $\{\alpha_n, \tau_n, \varphi_n\}$ being respectively the amplitude, excess time delay and phase shift and N the number of multipath components. As the time variation of the triplet is very slow when compared with the symbol time of the expected transmission rates, the channel can be considered constant for many symbol time periods, thus (9) can be written as

$$h(\tau) = \sum_{n=0}^{N} \alpha_n \delta(\tau - \tau_n)e^{j\varphi_n} \qquad (10)$$

The objective of a channel model is to obtain $\{\alpha_n, \tau_n, \varphi_n\}$. The statistical models try to approximate the statistical behavior of these three variables based on experimental measurements. As the practical channel sounders does not have an infinite bandwidth to discriminate all multipath components, the excess time delay variable is divided in time bins. Each time bin can have one or more multipath components which sum vectorially, resulting in a random variable given by

$$\alpha_n e^{j\varphi_n} = \sum_i \alpha_{n_i} e^{j\varphi_{n_i}} \qquad (11)$$

The amplitude distribution depends on the environment and on the used antenna configuration. The most popular distribution functions are: Rayleigh, Rice, Nakagami and lognormal [18]. The Poisson distribution have been generally used for the excess time delay, however its modified version is seen as the most appropriate. The phase shifts are generally assumed as uniformly distributed in the interval $[0, 2\pi]$, but the phase modeling of each component of the $h(\tau)$ as function of the mobile movement is seen as the most appropriate[18][19].

The DS parameter indicates the potential ISI that limits the carrier bit rate in TDMA (Time Division Multiple Access) systems. Measurements in several buildings reveals that this parameter is very dependent of the dimensions and building type, if exists line-of-sight (LOS) or not, the used antennas, etc.. Values between 20 and 50 ns were measured in small and medium size offices; between 30 and 300 ns in fabric environments; between 120 and 200 ns in big offices. However, similar values were obtained in small and big offices, which shows the influence of the construction materials of the buildings[21].

The channel characterization through the $h(\tau)$ gives the information of the received power level and the time dispersion which enables the evaluation of system performance. While $h(\tau)$ characterizes the channel at microscopic level, it is also useful to have a model at macroscopic level to evaluate the signal attenuation between the base station (BS) and the mobile terminal (MT). This information is essential for cellular planning. Several channel models to estimate the averaged received power level have been proposed. The simplest one follows the law $P(d) = P_0 d^{-n}$, where n depends on the environment. Also, the atmospheric and weather conditions have to be taken into account, specially for high frequencies, such as the 60 GHz band where the oxygen absorption is significant[22].

Based on what was mentioned above, the conclusion is that exists a certain number of possible distributions to model the radio channel and the use of one another depends on the propagation environment and the antenna configuration. On the other hand, a statistical model is conclusive only if it is based on a sufficient amount of data. When the number of parameters to be tested is high, the measurement campaigns become long and followed by a time consuming processing task, but the results are even more unfair due to the fact that these models are only valid for the conditions of the measurements and do not express any environment influence. This means that a model able to take into account a physical description of the propagation scenario, even a simplified one, is more efficient due to its general application.

Recently, a number of papers dealing with ray-tracing techniques to model the radio channel have been published. These techniques use a physical description of the propagation scenario and have shown a good agreement with measurements [6][23]-[26]. This fact combined with today computational capabilities, they have been proposed as suitable techniques for narrow and wide band radio channel modeling.

A. *Implementation of deterministic models*

A deterministic channel model should establish a physical relation between the propagation scenario and the parameters that characterize the channel impulse response. The model should also include the effects of the transceiver antennas and other changes in the scenario.

The high frequency approximation techniques are seen as the most appropriate to model the electromagnetic wave propagation behavior in the mmw region, once it can be described, with a reasonably accuracy, trough the use of geometrical optics (GO) principles, where each wave is represented by a ray.

A signal propagates through multiple paths, and therefore, the receiver antenna receives multiple replicas of the transmitted signal, which are delayed and attenuated differently. A ray can be affected cumulatively by several propagation mechanisms and its amplitude can be expressed by the following equation:

$$\alpha_n = C\left|\frac{\vec{E}(\theta_{Tn},\phi_{Tn})}{r_n}\underline{A}.\vec{l}_e(\theta_{Rn},\phi_{Rn})\right| \qquad (12)$$

with

$$\underline{A} = \underline{A}_s(\zeta_n)\underline{A}_D(\Theta_n)\prod_k \underline{R}(\gamma_{ik})\prod_j \underline{T}(\gamma_{ij}) \qquad (13)$$

r_n is the ray-path length, $\vec{E}(\theta,\phi)$ represents the electric field vector of the transmitting antenna at ray departure direction and $\vec{l}_e(\theta,\phi)$ the effective length of the receiving antenna; θ and ϕ are directional angles defined as in spherical co-ordinates where the subscript *T* stands for transmitting and *R* for receiving ray direction; $\underline{A}_S(\zeta_n)$ and $\underline{A}_D(\Theta_n)$ represent the attenuation due to scattering and diffraction effects, respectively, as a function of the angle; $\underline{R}(\gamma_{ik})$ and $\underline{T}(\gamma_{ij})$ represent, respectively, the reflection and transmission loss coefficients which depend on the incidence angle and on the materials properties. The eq. (12) can be seen as the Friis formula applied to each ray including the additional losses to the free space. Neglecting the losses introduced by the antennas, the constant C ($=\lambda/4\pi$) can be obtained through the Friis formula for free space propagation.

The phase and the excess time delay of each ray are given by (14) and (15) respectively.

$$\varphi_n = \arg\left\{\vec{E}(\theta_{Tn},\phi_{Tn})\underline{A}.\vec{l}_e(\theta_{Rn},\phi_{Rn})\right\} \qquad (14)$$

$$\tau_n = (r_n - r_0)/c \qquad (15)$$

where r_0 is shortest ray path and c the light speed in free space.

The channel modeling consists in tracing all possible rays between the transmitter and receiver and to calculate the losses and phase shift associated to each effect[26][27]. There are two main techniques to trace the ray-paths: the image method and the ray launching. From the last one, two versions can be derived, the ray splitting and the variation method to ensure the spatial resolution [28]. A ray-tracing tool, based on image method, was implemented and validated with measurements obtained in the 60 GHz band in several environments and with different antenna configurations [6][26].

III. SIMULATION RESULTS AND COMPARISON WITH MEASUREMENTS

Measurements and the corresponding simulations performed in several indoor environments have proved the validity of the ray-tracing tool. The results shown here were obtained in four rooms described below, with two different channel sounders employing different techniques, but more can be found in [26].

The Room A has approximate dimensions of 11.3m x 7.3m x 3.1m. One shorter wall consists of glass windows and the others consist of smoothly plastered concrete. The floor is linoleum on concrete and the ceiling consists of plastic plates encased in aluminum frames and lighting holders.

The Room B has approximate dimensions of 9.9m x 8.7m x 3.1m. One side wall consists of large floor to ceiling double-glazed windows encased in a steel frame while the other side walls are smooth metallic walls. The concrete floor is covered with thin carpet and the ceiling is made of aluminum profiles with lighting armatures. Wooden chairs and tables with metal legs are lined up through the room.

The Room C has approximate dimensions of 8m x 4m x 3.4m. The walls and ceiling panels are metallic and the concrete floor is carpeted. This room has a number of objects, mainly metallic.

The Room D is approximately rectangular with dimensions of 24.3m x 11.2m x 4.5m. One long side wall is completely windowed with double thermopane glass in a steel framework. The other walls are mainly made of wood. The concrete floor is covered with carpet and the ceiling is a complex structure made of plastic below the concrete.

The Fig. 2 depicts a typical measured and simulated PDP in the room D with a biconical horn, with a 10º degrees beamwidth in the vertical plane, at both stations. It is worth to see the good agreement between the amplitude and excess time delays of the measured and simulated main components of the PDP and of the cumulative delay spread. This also shows the very low contribution of the weaker components of the measured PDP when compared with nulls of the simulations. This is a very important conclusion, once it allows to neglect small contributions from diffraction and scattering effects and to simplify the physical description of the propagation scenario speeding up the simulation time.

Although the Rooms A and B have approximately the same dimensions, the NRP and time dispersion parameters are significantly higher in Room B as shown in Fig. 3. This is due to the reflection properties, once the Room B has three metallic walls while in Room A they are made of concrete. These results were also obtained with a pair of biconical horn antennas which give an approximately uniform coverage power level in the rooms. This is due to the figure eight shape of the antennas that compensates the higher free space attenuation of the longer rays, as illustrated in Fig. 5.

The Fig. 4 depicts the results obtained in Room C with two different antenna configuration. The Bic-Bic means that the BS and the MT uses a biconical horn antenna, but these ones have the radiation pattern tilted in the vertical plane: downwards at the BS and upwards at

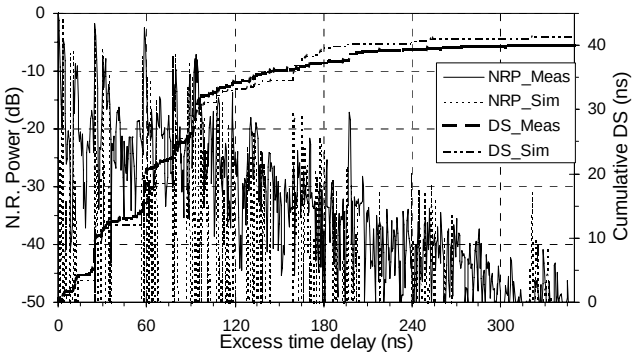

Fig. 2 Typical measured and simulated PDP and cumulative DS obtained in Room D

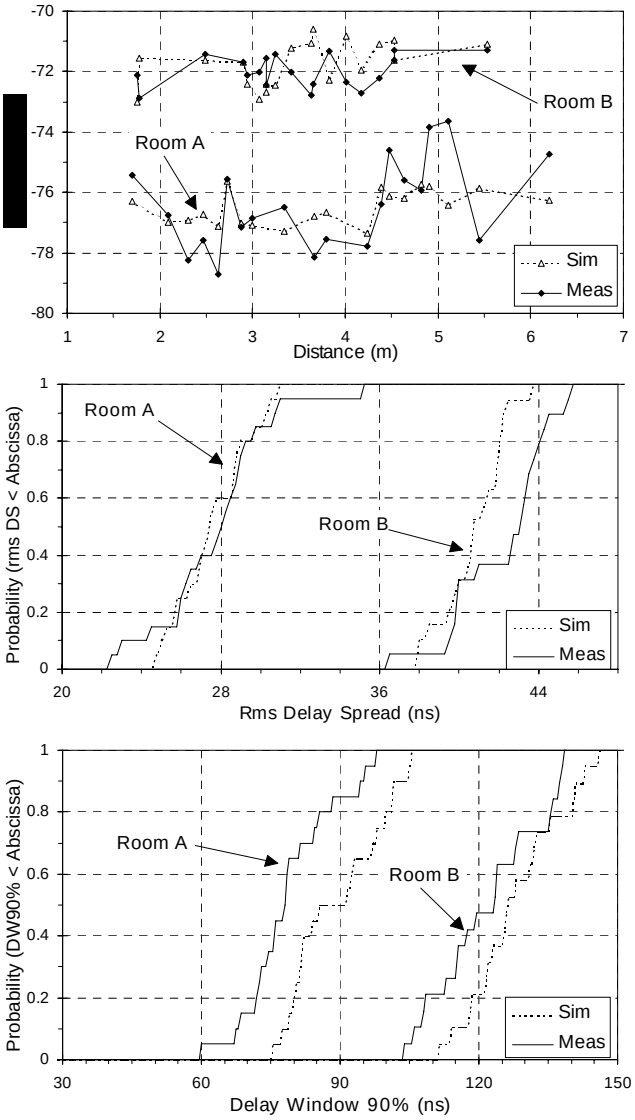

Fig. 3 Measured and simulated NRP, rms DS and DW90% in Room A and Room B

MT. The Horn-Bic means that the BS uses a horn antenna (pyramidal) and the MT uses the same biconical antenna. Although the lateral walls and ceiling are metallic, the time dispersion parameters are significantly lower than in the Rooms A and B, as it can be observed in Fig. 4. This is partially due to the shorter dimensions of the room and to the umbrella shaped antenna radiation patterns. It can also be seen the reduction of time dispersion obtained with the pyramidal horn antenna at the BS. These examples clearly show the impact of the antenna configuration and the environment on the propagation channel parameters [26].

In order to give some insight on the variation of the time dispersion parameters with antenna configuration, room dimensions and reflective index, it is represented in Table 1 the values of the rms DS and DW90% that are not exceeded in 50% and 90% of the cases. These values are directly obtained from the cumulative distribution functions of the respective parameter[26].

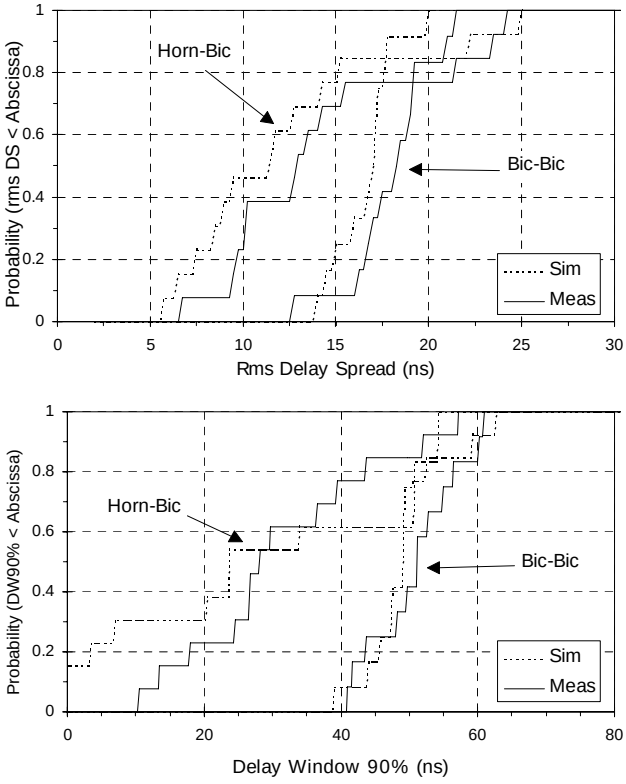

Fig. 4 Measured and simulated rms DS and DW90% in Room C with Bic-Bic and Horn-Bic antenna configuration

IV. ANTENNA CONFIGURATIONS

As we have seen in Sec.III, the antenna configuration has a direct impact on the channel impulse response, therefore, they have to be chosen so as to provide the best system performance. In this context, they should provide a good power distribution in the covered area and low time dispersion in order to enable the high carrier bit rates.

In what concerns the movement freedom of the mobile terminal, the omni-directional antenna would the obvious candidate, but it offers the worst gain characteristics. On the other hand, the directive antennas can offer a high gain and be effective in combating the channel time dispersion, but they limit the movement freedom. The best way is to combine the advantages, which can be done by resorting to adaptive antennas,

either switchable beams (sectored antennas) or adaptive arrays [26].

The configuration with a pair of biconic horn antennas provide an almost uniform power level distribution, but the time dispersion is quite high, which makes it suitable only for small environments, see Fig. 5. Other possibility is to use two horn antennas at the BS located in the center of the narrower lateral walls of the room, see Fig. 6. The beamwidth (BW) and the orientation in azimuth and elevation planes of any of the BS antennas are chosen to cover directly 2/3 of the room. They are similar but one antenna uses a different carrier frequency from the other located on the opposite side of the room. These two antennas can be connected to each other by optical fiber using the MODAL (Micro-wave Optical Duplex Antenna Link) concept[29].

Table 1 Time dispersion parameters in different rooms

Room	Dimensions (m)	Reflective index	Antenna configuration	rms DS (ns) 50%	rms DS (ns) 90%	DW90% (ns) 50%	DW90% (ns) 90%
A	11.3x7.3x3.1	medium	Bic-Bic	28	31	78	95
B	9.9x8.7x3.1	very high	Bic-Bic	42	44	125	138
C	8.0x4.0x3.4	very high	Bic†-Bic†	18	21	50	60
			Horn-Bic†	12	24	28	52
D	24.3x11.2x4.5	low	Bic-Bic	42	46	125	146
			Horn-Bic	25	54	60	157
E	12.9x8.9x4.0	very low	Bic-Bic	19	23	51	67
F	13.0x7.0x3.4	high	Bic†-Bic†	15	17	33	50
			Horn-Bic†	9	16	19	29
G	13.0x3.4x3.4	high	Bic†-Bic†	16	22	20	50
H	12.0x7.0x3.4	medium	Horn-Bic†	6	11	13	23

† These are umbrella shaped biconic horn antennas

The configuration with a pair of biconic horn antennas provide an almost uniform power level distribution, but the time dispersion is quite high, which makes it suitable only for small environments, see Fig. 5. Other possibility is to use two horn antennas at the BS located in the center of the narrower lateral walls of the room, see Fig. 6. The beamwidth (BW) and the orientation in azimuth and elevation planes of any of the BS antennas are chosen to cover directly 2/3 of the room. They are similar but one antenna uses a different carrier frequency from the other located on the opposite side of the room. These two antennas can be connected to each other by optical fiber using the MODAL (Micro-wave Optical Duplex Antenna Link) concept[29].

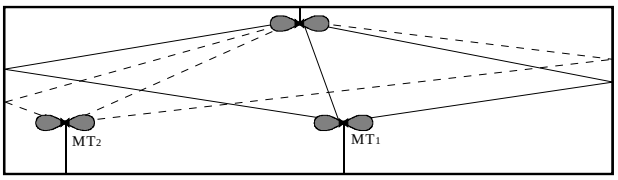

Fig. 5 Antenna configuration using biconic horns at BS and MT

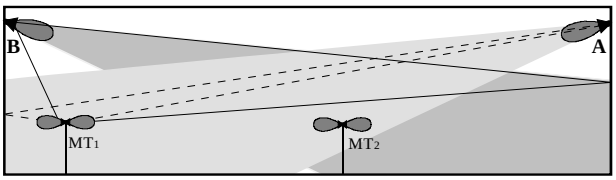

Fig. 6 Antenna configuration using two horns at BS

Simulation results for these two main antenna configurations are presented in Fig. 7 and Fig. 8 with different antennas in the MT, namely a biconical horn with a BW of 30º in the vertical plane, a 6 sector antenna with a vertical BW of 30º having a 3 dB horizontal BW of 60º within each sector, and several linear and planar arrays. A radiation pattern identical to the biconical horn was assumed for the array elements, all of them identical, for comparison purposes. The relatively large BW chosen for the vertical plane is to provide sufficient movement freedom. All antennas were vertically polarized [30].

The Fig. 7 depicts the NRP as a function of distance between BS and MT antennas, and the cumulative distribution function (CDF) of the rms DS and DW90% for a centrally placed BS and different antenna types at the MT in Room D. The curve labeled *S6-S6* means that

both BS and MT use a six sector antenna. The active pair of sectors to establish the communication is chosen based on higher received power level. The other curves in this figure correspond to a different antennas at the MT and a biconical horn centrally placed in the room as a BS antenna. In the figure legend, *Bic* means that the MT antenna uses a biconical horn; *L9, L16, L36* represents a linear array of 9, 16 and 36 elements; *R4x4* is a rectangular array with 16 elements in a grid of 4 by 4, and finally *S6* is six sector antenna.

Higher NRP values are obtained either with a pair of six sector antennas or with the linear array *L36* at the MT, but the pair of sectored antennas presents lower time dispersion. This was the expected performance once these two sets are the most directive. The lower NRP at

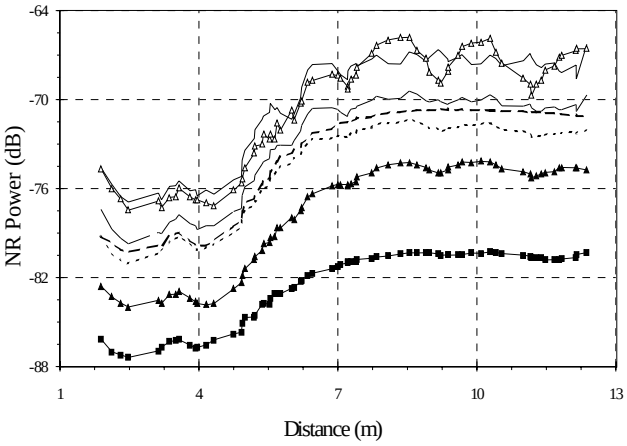

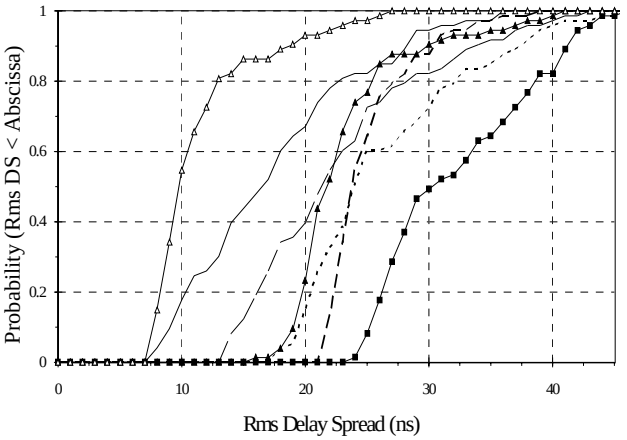

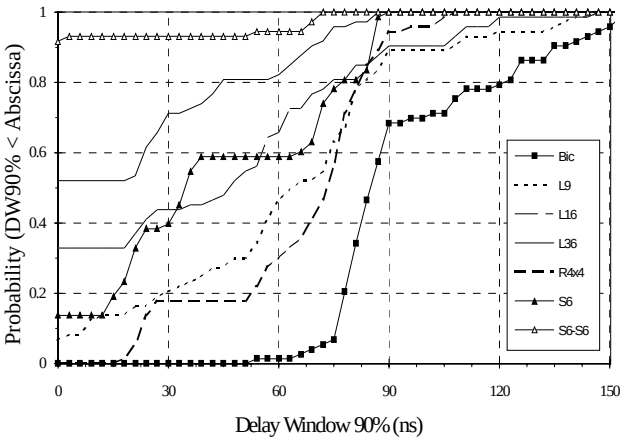

Fig. 7 NRP as a function of distance BS and MT, CDF of rms DS and of the DW90% in room D with the BS centrally placed.

shorter distances is due to the figure eight shape of the biconical horn which favors the further than the closer positions.

The 16 elements linear array offers better performances than a rectangular array of the same number of elements. The rectangular array allows steering in azimuth and elevation planes, but it provides a wider beamwidth. As in this type of environments, and particularly with a biconical horn at the BS, the steering in the elevation plane has no major importance once the

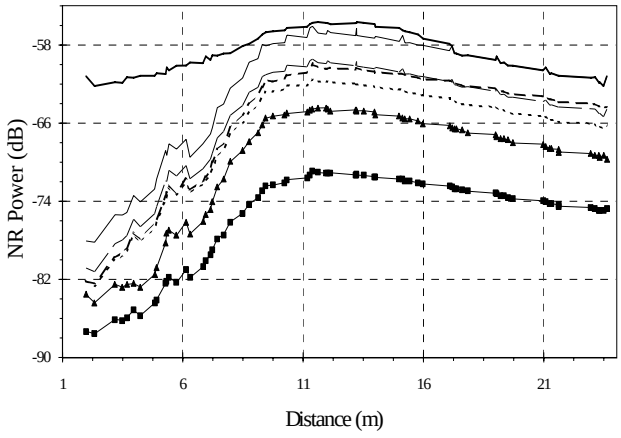

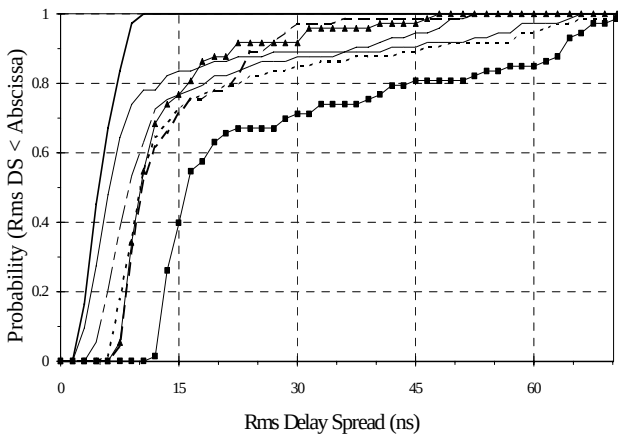

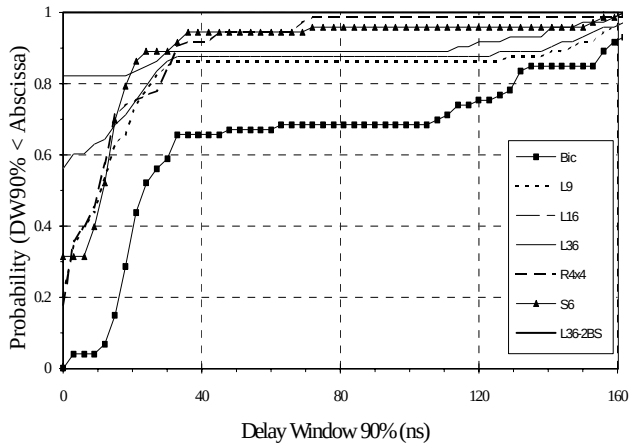

Fig. 8 NRP as a function of distance BS and MT, CDF of rms DS and of the DW90% in room D with the BS laterally placed.

most significant multipath components are generally received at low elevation angles.

A similar performance improvement can be observed in Fig. 8 corresponding to the same room but with the BS antenna laterally placed. This antenna exhibits a BW of 7º and 70º respectively in the elevation and azimuth planes, and is rotated 6º below the horizontal plane. The full room coverage is made with two identical BS antennas. In this figure, only the curve labeled *L36-2BS* represents the results considering the two BS antennas, the others correspond to only one antenna. This is to show the results obtained with one BS antenna and the reader can easily infer the results when the two BS antennas are used.

The time dispersion parameters in Fig. 8, in more than 60% of the cases, have significant lower values which complies with the higher NRP values for distances above 8-9 meters. This corresponds to the area covered directly by one BS antenna. The possibility that the MT has of choosing one between the two BS transceiver antennas, reduces significantly the overall time dispersion parameters as well as the NRP dynamic range. This is illustrated in Fig. 8 in case the MT uses a linear array of 36 elements (*L36-2BS*). Fast fading was removed from the results to make the figures more clear.

V. EVALUATION TRANSMISSION PERFORMANCE

In digital transmission over narrow-band radio channels, the time dispersion of the channel is small when compared with the symbol period. In this case, the main error mechanism is the envelop fading. For broadband transmissions, the channel time dispersion can span over several number of symbol periods, which causes ISI. Using an equalizer at the receiver, the ISI can significantly be reduced and the bit error rate (BER) improved.

At high signaling rates, the time dispersion introduced by the channel can be considered a form of frequency diversity at the receiver. This is because the signal bandwidth is much larger than the average fade bandwidth, and only a small part of the signal spectrum will be faded at one time. This signal diversity will limit the depth of envelope fading at the receiver. As the symbol rate is reduced, the signal bandwidth narrows and, if it becomes comparable with fade bandwidth, a single fade can attenuate a large portion of the signal spectrum, causing envelope fading.

In a large database of frequency-domain measurements, the envelope of a signal with 100 MHz bandwidth was not observed to fade below 9 dB of its average, while for a signal with 1 MHz bandwidth was observed to fade below 30 dB [31]. These results indicate that the time dispersion at high signaling rates provides some form of diversity reducing the envelop fading. However, if the time dispersion becomes too large an irreducible error rate due to the ISI is achieved, for a certain equalizer configuration. The higher the equalizer depth (e.g., more taps), the higher time dispersion is able to handle. Since the time dispersion of the radio channel is greatly influenced by the used antenna configuration, it appears that the maximum transmission capacity in an environment strongly depends on the antenna configuration and the employed equalization effort [7].

The Fig. 9 and Fig. 10 depict some transmission performance results obtained in Room D by using the 4-OQAM modulation scheme and a Decision-feedback equalizer (DFE) in the receiver. The transceiver specification are identical to those described in [32] and only uncoded transmission from BS to MT has been considered. An average BER was evaluated for each MT spot position, by Monte-Carlo simulation, for a set of a thousand simulation bursts, with the corresponding thousand channel impulse responses obtained with the ray tracing tool around each MT spot position within the room.

The simulation results in Fig. 9 and in Fig. 10 show the global radio transmission performance along the room for the two basic antenna configuration (see Fig. 5 and Fig. 6), with a 7 taps in both filters of the equalizer and a BER = 10^{-3} [7]. Each curve in the figures corresponds to a different position of the MT, and represent the best and the worst case, the highest and the lowest achievable carrier bit rate (CBR).

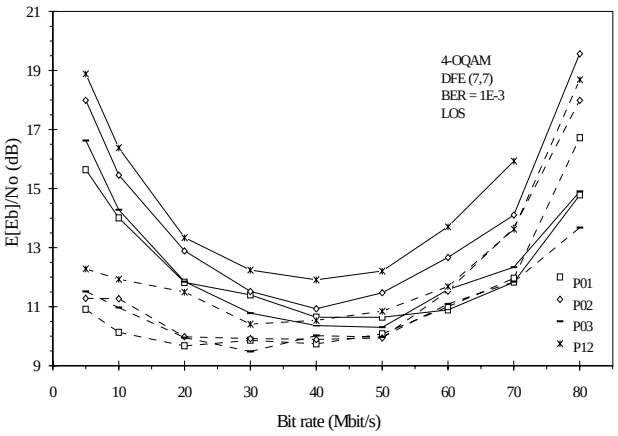

Fig. 9 Required $E[Eb]/No$ as a function of CBR for a centrally placed BS and a biconical horn at MT in four different positions (DW_{P01}=90 ns, DW_{P02}=100 ns, DW_{P03}=100 ns, DW_{P12}=140 ns).

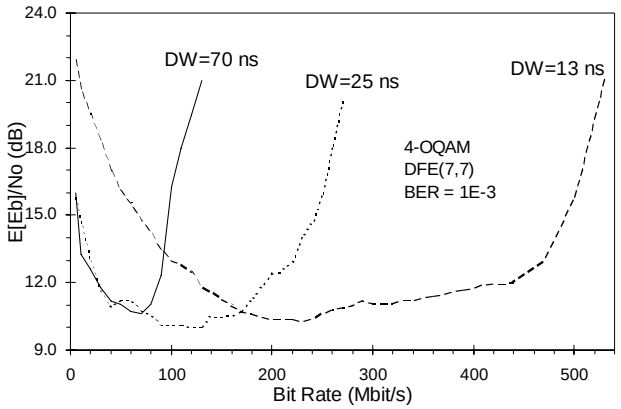

Fig. 10 Required $E[Eb]/No$ as a function of CBR for a laterally placed BS and a biconical horn at MT in three different positions.

It can be observed in Fig. 9 that as the bit rate increases above 40-50 Mbit/s, the required $E[Eb]/No$ increases. The main error mechanism in this range is the ISI, because the symbol time period becomes shorter, decreasing the equalizer depth, leading to a higher ISI. On the other hand, the required $E[Eb]/No$ increases as CBR decreases below 30-40 Mbit/s. In this range, the main error mechanism is envelope fading because the symbol time gets larger (the signal spectrum bandwidth narrower) and the intrinsic frequency diversity effect observed at high signaling rates becomes negligible. Another effect which confirms this mechanism, is the significant improvement obtained with antenna diversity (dotted lines) for lower bit rates. It seems that decreasing the bit rate below 5 Mbit/s, $E[Eb]/No$ will tend to theoretical values under flat fading situation, 13.5 dB with diversity and 24.5 dB without diversity.

Fig. 10 represents the transmission performance for three MT positions and demonstrates that it is significantly different from each other, the coverage is not so uniform as it is with a pair of biconical antennas. As these three positions represent the best and worst cases in the coverage area of the BS antenna, it can be concluded that a minimum CBR of 100 Mbit/s is guaranteed, and in some positions it can reach 500 Mbit/s. This clearly illustrates the influence of the antenna configuration on propagation channel parameters (e.g., the value of DW ranges from 13 to 70 ns) and on the transmission performance (CBR ranges from 100 to 500 Mbit/s)

The performance improvement of this antenna configuration becomes even more evident if we compare the required transmitted power. Considering a receiver with a noise figure of 10 dB and a CBR of 40 Mbit/s, the required transmitted power is 10 dBm for the configuration that uses two biconic horns, while it reduces to 3 dBm with the laterally placed horn antennas [26].

Several signal processing techniques can be employed in order to increase the upper limit imposed on bit rate due to multipath propagation, but they can not cope, either due to cost and/or complexity, with very large channel time dispersion. It appears that the best solution is to use an adequate antenna configuration in order to reduce the time dispersion and the required transmitted power combined with a moderate equalization effort.

A. *Estimation of the equalization depth*

The channel time dispersion causes ISI and in the limit imposes an irreducible BER. As we have seen before, the higher the time dispersion the lower is the bit rate per carrier. One important issue is to relate the channel time dispersion with the achievable bit rate per carrier, but for that we need to estimate the equalization depth based on equalizer configuration, e.g., the number of taps and the space between them.

The Fig. 11 depicts part of the simulations performed using a DFE(N, M), for different values of N and M, respectively the number of taps in the forward and in the feedback filter. This figure shows that, for the same $E[Eb]/No$, the bit rate increases with the number of taps of the DFE. Thus, the required transmitted power level is the same, while the complexity of the equalizer is increased.

For the same $N + M$ the performance characteristics are different: with a DFE(N, M) where $M > N$ and other DFE(N', M') with $N' > M'$ and $N + M = N' + M'$, the first configuration performs better. Since $M \geq N$ the equalization depth (Ed) can be approximated by

$$Ed = \frac{N + M}{2} TSp \qquad (16)$$

with TSp being the tap spacing of the equalizer filters, which is, generally, a fraction of the symbol time.

In case of $N > M$ the excess number of taps has nearly half of the effect as compared in the feedback filter, then

$$Ed = \frac{\left(M + \frac{N-M}{2}\right) + M}{2} TSp \qquad (17)$$

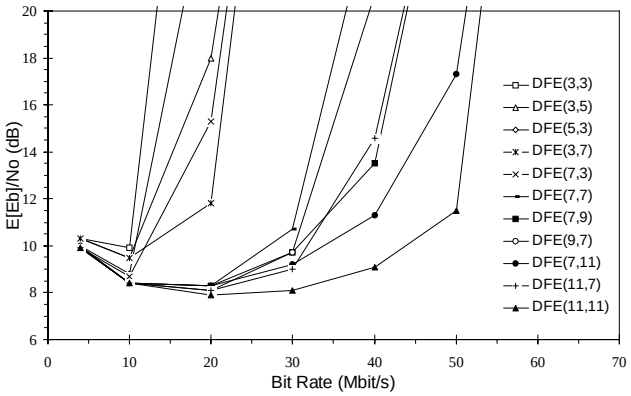

Fig. 11 $E[Eb]/No$ as a function of carrier bit rate for different values of N and M.

$$Ed = \left(\frac{3}{4}M + \frac{1}{4}N\right) TSp \qquad (18)$$

Once we know the equalization depth, the carrier bit rate can be estimated trough the DW parameter, which must be lower than the equalization depth.

VI. TECHNOLOGICAL ASPECTS

The world-wide activities on MMIC (Monolithic Microwave/ Millimeter-wave Integrated Circuits) design are concentrated on single function MMICs. The transceiver development for the mmw band are mainly driven by the requirements for the fixed radio links at 38 and 55 GHz, where the size, weight and power consumption are not the major restrictions. Many of the existing equipment uses waveguide-based components, but the new developments are focusing on the use of multifunction MMICs.

A good circuit integration level, able to implement several functions, in order to reduce the size, weight and power consumption are clearly mandatory for the mobile terminals. The European foundries are already able to built circuits with a gate length less than 0.2 μm, which permits to achieve 1.5 dB noise figure at 40 GHz. In Japan, they already achieved 3.4 dB at 91 GHz with a gate length of 0.15 μm and 3.2 dB at 95 GHz with 0.1 μm in the United States.

In what concerns the base-band processing, the world-wide activities are concentrated on mass market operation, such as GSM and WLAN that require much lower bit rates. ASIC equalizers to operate at 100 MBaud have been realized for fixed links using the 1024-QAM modulation scheme, but they cannot be used in mobile radio systems due to the fading and time dispersion levels exhibited by the multipath radio channel. As the equalizers must be adaptive to mitigate the distortion effects introduced by the time variant channel, it requires high speed circuits with high integration level to implement the necessary functions, usually with a certain complexity to accommodate the very high bit rates. The basic functions to be implemented are channel coding/decoding, framing/ deframing, equalization, error detection and correction, etc..

The industry can achieve an integration of 1000 kgates (1 million gates) with CMOS technology providing a delay time of 120 ~ 300 ps, a power dissipation of 0.5 ~ 1 μW/MHz.gate (with a possibility of dissipating 5 W with ceramic encapsulating) and a clock speed of 200 MHz. With GaAs technology it is possible to go up to 3 GHz by reducing the integration level down to 100 kgates but improving the time delay to 100 ps.

VII. CONCLUSIONS

A general description of the mobile radio channel was presented and the multipath propagation phenomena identified. The main implementation issues of a deterministic model, using ray-tracing techniques, were outlined.

A comparison of the ray-tracing simulation results with measurements was made and a very good agreement observed. From these data, emerges the conclusion that the characteristics of the radio channel depends very much on the antenna configuration and on the propagation environment.

Some system simulations were presented in order to show the impact of the radio channel on the broadband transmission performance. The carrier bit rate is directly related with the channel time dispersion, namely with the DW parameter. From this parameter it is possible to estimate the carrier bit rate once we know the equalization depth which is related the number of taps of the equalizer. This means that the very high bit rates can be achieved with a high equalization depth or with an antenna configuration that gives a channel impulse response with low time dispersion. However, the best solution seems to be the use of an equalizer with moderate complexity and an adequate antenna configuration sharing the task of time dispersion mitigation. As movement freedom of the mobile terminal, gain and multipath discrimination are opposite requirements, the best compromise can be achieved by resorting to adaptive antennas. Due to the implementation costs, the sectored antennas seem to be preferable relatively to the array antennas.

It can be concluded that with a low equalization effort it is possible to achieve some tens or even hundreds of Mbit/s provided the adequate antenna configuration for the environment is chosen. This wide-band transmission rate will enable the extension of the broadband services available at the B-ISDN to the mobile users.

VIII. REFERENCES

[1] L. Fernandes, "*Developing a System Concept and Technologies*

for Mobile Broadband Communications", IEEE Personal Communications Magazine, Feb. 1995.

[2] J. S. Dasilva, B. Arroyo, B. Barani, D. Ikonomou, "*European Third Generation Mobile Systems*", ACTS Mobile Telecom. Summit, Granada, Spain, Nov. 1996.

[3] A. Robert et. al., "*Australian Activities in Microwave Links for Wireless LANs*", IEEE MTT-S International Microwave Symposium, Atlanta, Georgia, CSIRO Division of Radiophysics, 1993.

[4] D. Falconer "*Broadband Indoor Wireless Commu-nications*", Proposal for a major Project of the citr., CITR, Dept of Systems and Computer Engineering, Carleton University, June 1993.

[5] M. Umehira, M. Araki e T. Murase, "*Overview of Wireless LANs in Japan*", ACTS Mobile Communications Summit, Aalborg, Denmark, 1997.

[6] J. Fernandes, P. Smulders and J. Neves, "*Mm-wave Indoor Channel vs. Measurements*", Wireless Personal Comm. Journal, Vol. 1, No 3, pp. 211-219, 1995

[7] J. Fernandes, J. Nascimento, A. Gusmão, R. Dinis and J. Neves, "*Performance Evaluation of Mm-wave Wide-Band Digital Radio Transmission*", IEEE 2nd Symposium on Comm. and Vehicular Technology in the Benelux, Nov. 1994.

[8] R. Dinis, A. Gusmão and J. Fernandes, "*Performance Evaluation of Equalisation/ Diversity Schemes for MBS*", RACE Mobile Telecommunications Summit, Cascais, Portugal, Nov. 1995

[9] P.F.M. Smulders, and A.G. Wagemans, "*Wideband Indoor Radio Propagation Measurements at 58 GHz*", Elect. Letters, Vol. 28, No 13, pp. 1270-1272, Jun 1992.

[10] G. Lovnes, J. Reis and R. Raekken, "*Channel Sounding Measurements at 59 GHz in City Streets*", PIMRC '94, The Hague, The Netherlands, Sept. 1994.

[11] H. Thomas, R. Cole and G. Siqueira, "*An Experimental Study of the propagation of 55 GHz Millimeter Waves in an Urban Mobile Radio Environment*", IEEE Trans. on Vehicular Technology, Vol. 43, No 1, Feb. 1994.

[12] M. Bensebti, J.P McGeehan and M.A. Beach, "*Indoor Multipath Radio Propagation Measurements and Characterization at 60 GHz*", Proc. 21st European Microwave Conf., pp. 1217-1222, Sept. 1992.

[13] C. Ciotti and J. Borowski, "*The AC006 MEDIAN Project - Overview and State of the Art*", ACTS Mobile Telecomm. Summit, Granada, Spain, Nov. 1996.

[14] G.A. Kalivas, "*Millimeter-Wave Channel Measurements with Space Diversity for Indoor Wireless Communications*", IEEE Trans. on Vehic. Technology, Vol. 44, No 3, Aug. 1995.

[15] E. Damosso (Editor), "*Digital Mobile Radio: COST 231 View on the Evolution Towards 3rd Generation System*", COST 231 Final Report, 1996.

[16] P.A. Bello, "*Characterization of Randomly Time-Variant Linear Channels*", IEEE Trans. on Communications Systems, CS-11, pp. 360-393, 1963.

[17] J.D. Parsons, "*The Mobile Radio Propagation Channel*", Prentech Press, London, 1992.

[18] H. Hashemi, "*The Indoor Radio Propagation Channel*", Proc. of the IEEE, Vol. 81, No 7, pp. 943-968, July 1993.

[19] P. Marques, J. Fernandes and J. Neves, "*Complex Impulse Response Modeling for Wideband Radio Channels*", 48th Vehicular Technology Conference, Ottawa, Ontário, Canada, May 1998. To be published.

[20] J. Proakis, "*Digital Communication*", 2nd edition, McGraw-Hill, 1989.

[21] D. Desvairvatham, "*A Comparison of Time Delay Spread and Signal Level Measurements Within Two Dissimilar Office Buildings*", IEEE Trans. Antennas and Propagation, Vol. 35, No 3, pp. 319-324, March 1987.

[22] L. Correia , J. Reis and P. Francês, "*Analysis of the Average Power to Distance Decay Rate at the 60 GHz Band*", VTC'97.

[23] C. Peter Ho, T. Rappaport, M. Koushik, "*Antenna Effects on Indoor Obstructed Wireless Channels and a Deterministic Image-Based Wide-Band Propagation Model for In-Building Personal Communication Systems*", Int. Journal of Wireless Information Networks, Vol. 1, No 1, 1994.

[24] S. Seidel and T. Rappaport, "*A ray Tracing Technique to Predict Path Loss and Delay Spread Inside Buildings*", Proc. IEEE GLOBECOM '92 Conf., Orlando, Florida, pp. 649-653, Dec. 1992.

[25] T. Holt, K. Pahlavan and J.F. Lee, "*Ray Tracing Algorithm for Radio Propagation Modeling*", Proc. 3rd IEEE Int. Symp. Personal, Indoor and Mobile Radio Communications, Boston, Mass., Oct. 1992.

[26] J. Fernandes, " *Modelização do Canal de Propagação Rádio Móvel de Banda Larga na Faixa das Ondas Milimétricas e seu Impacto no Desempenho de Transmissão do Sistema*", PhD Thesis, Universidade de Aveiro - DETUA (in Portuguese), 1996.

[27] P.F.M. Smulders and J. Fernandes, "*Wide-Band Simulation and Measurements of Mm-wave Indoor Radio Channels"*, PIMRC '94, The Hague, The Netherlands, Sept. 1994.

[28] T. Huschka, "*Ray Tracing Models for Indoor Environments and their Computational Complexity*", PIMRC '94, The Hague, The Netherlands, pp. 486-490, Sept. 1994.

[29] R. Heidemann et. al.,"*Remoting of UMTS- and MBS- Antenna by Fibre Optic Technology*", RACE Mobile Workshop, Amsterdam, May 1994.

[30] J. Fernandes, O. Sousa and J. Neves, "*Impact of Antenna Set-up and arrays on Mobile Radio Systems*", 4th Int. Conf. on Universal Personal Communications (ICUPC'95), Japan, 1995

[31] M.R. Gibbard, G. Morrison, A. Seasy and M. Fattouche, "*Broadband TDMA over the Indoor Radio Channel*", Electronics Letters, Vol. 30 No 4, Feb. 1994.

[32] A. Gusmão, J. Fernandes and Rui Dinis, "*Performance of MBS Radio Transmission*", RACE Mobile Workshop, Amsterdam, May '94.